frontiers in Medicine

TYPE Original Research
PUBLISHED 06 November 2026
DOI 10.3389/fmed.2026.1914546

Check for updates

OPEN ACCESS

EDITED BY
Raffaele Simeoli,
IRCCS, Italy

REVIEWED BY
Tuuli Metsvaht,
University of Tartu, Estonia
Achmad Rafli,
University of Indonesia, Indonesia
Zhou-Jie Liu,
First Affiliated Hospital of Fujian Medical University, China

*CORRESPONDENCE
Xukun Liao
kkingbeast@163.com
Zijun Yan
swallowyzj@163.com

RECEIVED 20 June 2026
REVISED 24 October 2026
ACCEPTED 27 October 2026
PUBLISHED 06 November 2026

CITATION
Liao X, Zhang L, Cheng J, Song F and Yan Z (2026) Development of a machine learning-based treatment-response prediction model for levetiracetam in pediatric epilepsy: integrating ABCB1 polymorphism and therapeutic drug monitoring.
Front. Med. 13:1914546.
doi: 10.3389/fmed.2026.1914546

COPYRIGHT
© 2026 Liao, Zhang, Cheng, Song and Yan. This is an open-access article distributed under the terms of the Creative Commons Attribution License (CC BY). The use, distribution or reproduction in other forums is permitted, provided the original author(s) and the copyright owner(s) are credited and that the original publication in this journal is cited, in accordance with accepted academic practice. No use, distribution or reproduction is permitted which does not comply with these terms.

Development of a machine learning-based treatment-response prediction model for levetiracetam in pediatric epilepsy: integrating ABCB1 polymorphism and therapeutic drug monitoring

Xukun Liao[1]*, Liangming Zhang[1], Jingdong Cheng[1], Fangyu Song[1,2] and Zijun Yan[1]*

[1]Department of Pharmacy, Panzhihua Central Hospital, Panzhihua, China, [2]School of Pharmacy, Dali University, Dali, China

Background: Empirical dosing of levetiracetam (LEV) in pediatric epilepsy often yields variable outcomes. This study aimed to develop a machine learning-based treatment-response prediction model integrating therapeutic drug monitoring (TDM) and ABCB1 C3435 T polymorphism.
Methods: Clinical, TDM, and genetic data from 346 pediatric patients were retrospectively analyzed. Four machine learning algorithms were evaluated. SHapley Additive exPlanations (SHAP) was utilized to interpret feature associations.
Results: The XGBoost model demonstrated the highest predictive performance (AUC=0.893). SHAP analysis indicated that LEV trough concentration (C_{min}) and ABCB1 genotype were the strongest associative factors for clinical outcomes. The homozygous TT mutation was associated with treatment resistance despite adequate peripheral C_{min}. SHAP interaction patterns generated an exploratory hypothesis that ABCB1 genotype may modify the associative relationship between systemic exposure and treatment response.
Conclusion: Integrating ABCB1 genotyping and TDM via the XGBoost model may provides an interpretable approach for predicting LEV treatment response in pediatric epilepsy. Rather than directly generating individualized dosing regimens, these associative findings offer a hypothesis-generating reference for identifying patients at risk of therapeutic failure, warranting further prospective exposure-response validation.

KEYWORDS
levetiracetam, machine learning, pediatric epilepsy, pharmacogenomics, therapeutic drug monitoring

1 Introduction

Due to its favorable pharmacokinetics, Levetiracetam (LEV) is a commonly used drug in paediatric epilepsy (1). However, inter-individual variability of drug metabolism and effect is substantial in children, and empirical weight-based dosing is difficult (2). Therapeutic drug monitoring (TDM) has been increasingly utilized to monitor with

peripheral steady-state trough concentrations to optimize drug dosages (3). Although it is useful, it is not always possible to keep concentrations in conventional reference ranges and prevent therapeutic failure or adverse events (4). Current clinical observations indicate that peripheral drug concentrations may not be sufficient to predict drug effects in this patient group (5).

One explanation for this difference in systemic and clinical response could be that these drugs are distributed by different mechanisms across the blood-brain barrier (6). P-glycoprotein, an efflux transporter encoded by the ABCB1 gene, has been hypothesized to influence the central nervous system penetration of various antiseizure medications (7). However, whether LEV is a definitive substrate of human P-glycoprotein remains incompletely established, as experimental studies have reported weak or species-specific transport *in vitro* despite evidence of P-gp interaction in animal models (8). Similarly, while genetic polymorphisms in ABCB1—particularly the C3435 T (rs1045642) variant—have been proposed to modulate P-glycoprotein expression and LEV disposition in certain pediatric cohorts, clinical findings remain conflicting and inconclusive. These controversies suggest that the impact of this polymorphism might not follow a simple linear pattern but could be influenced by multifaceted clinical contexts. Therefore, the interaction of different ABCB1 genotypes may lead to different exposures to the drug in the brain in patients who have similar blood concentrations of the drug, and the evaluation of pharmacogenomic factors might be performed together with TDM (9).

Complex non-linear interactions are involved in analysing the combined effects of genetic polymorphisms and pharmacokinetic parameters (10). For instance, a specific drug concentration might be therapeutically effective for one genotype but induce toxicity in another, representing a complex conditional logic and threshold effect. Multidimensional clinical data often exhibit these complex conditional relationships that are difficult to accurately model with traditional linear statistical approaches like logistic regression (11). Machine learning algorithms are a promising alternative because of their ability to capture non-linear relationships and combine multiple clinical characteristics. SHapley Additive exPlanations (SHAP) analysis can be used to overcome the opacity of machine learning (12). This approach provides the model predictions interpretability, and allows a clinician to see how different variables interact to affect results.

The purpose of this study is thus to investigate the population pharmacokinetics of LEV and the occurrence of ABCB1 C3435 T polymorphism in Chinese children with epilepsy. Importantly, rather than directly outputting a quantitative individualized dose regimen, this study aims to establish a treatment-response prediction framework that evaluates whether a patient is likely to respond under given clinical characteristics and systemic exposure levels, thereby generating exploratory hypotheses for future personalized therapy optimization.

2 Materials and methods

2.1 Study design and ethical considerations

The study was a retrospective observational study that included patient information from January 2019 to December 2025 from Panzhihua Central Hospital. This study was approved by the Institutional Review Board of Panzhihua Central Hospital [Approval No. (2026-012)]. Every human subject procedure was conducted in accordance with standard ethical guidelines regarding research with human subjects (1975 Declaration of Helsinki and its amendments). The ethics committee waived the need for written informed consent for the retrospective data collection and use of anonymized clinical records.

2.2 Patient selection criteria

Patients included in the study were those with epilepsy who were receiving levetiracetam (LEV) therapy. Inclusion criteria were: age less than 18 years (strictly); documented baseline seizure frequency over a 3-month observation period prior to LEV initiation; continuous administration of an initial stable maintenance dose of LEV for at least five to seven days to achieve steady-state pharmacokinetics prior to blood sampling; peripheral steady-state trough concentration (Cmin) collected within 0.5 h before the next scheduled dose; availability of ABCB1 C3435 T genotyping results; and a minimum post-TDM follow-up duration of 6 months under the maintenance regimen. Patients were excluded from the analysis if they had severe liver or renal dysfunction before LEV was initiated, or if medication adherence was poor based on medical records, or if complete demographic, laboratory or clinical follow-up data were not available.

2.3 Data collection and clinical variables

A common protocol of data extraction was used to obtain a set of multidimensional features per patient. Demographic and anthropometric parameters included age, sex, ethnicity, body weight, height and body surface area (BSA). Clinical and therapeutic variables included type of epilepsy (focal, generalized or unknown), type of therapy (monotherapy or polytherapy), concurrent use of specific anti-seizure drugs (valproic acid, oxcarbazepine or carbamazepine), formulation of drug administered (oral solution or tablet), number of doses/day, total dose/day, and dose/day/kg. Laboratory tests performed at baseline were serum alanine aminotransferase (ALT) and serum creatinine (Scr). The main experimental factors were LEV Cmin, CDRs (calculated concentration to dose ratio), and ABCB1 genotypes, which were divided into three groups, CC, CT, and TT. Because LEV exhibits linear, time-independent pharmacokinetics with minimal protein binding and no hepatic auto-induction, the initial steady-state Cmin reliably reflects maintenance systemic exposure provided that dosing adherence remains consistent. Consequently, excluding patients with poor medication adherence allowed the initial steady-state Cmin (measured after 5–7 days of stable maintenance dosing) to serve as a valid proxy for longitudinal exposure. Furthermore, to ensure a clear forward-looking temporal sequence and prevent reverse causality or temporal information leakage, only this initial steady-state Cmin measurement obtained prior to the outcome evaluation window and prior to any outcome-driven dose modification was included in the predictive model. Clinical

endpoints were subsequently assessed over a 6-month follow-up window using data extracted from the hospital's structured electronic medical record (EMR) system. As part of routine clinical care at our institution's pediatric epilepsy clinic, parents or legal guardians were instructed to maintain standardized daily seizure diaries. At scheduled monthly or bi-monthly outpatient follow-up visits, the attending pediatric neurologists reviewed these diaries and documented the monthly seizure frequency, medication adherence (verified via prescription refill records and caregiver inquiry), and treatment-emergent adverse events (assessed using a routine clinical checklist covering neuropsychiatric, behavioral, and somatic symptoms) directly into the EMR. Based on these longitudinal records, therapeutic response was defined as a $\geq 50\%$ reduction in average monthly seizure frequency during the 6-month follow-up period compared with the 3-month pre-treatment baseline period.

2.4 ABCB1 C3435 T genotyping analysis

The genomic DNA from 2 mL of peripheral venous blood samples of the patients was extracted by QIAamp DNA Blood Mini Kit (Qiagen, Hilden, Germany) according to the manufacturer's instructions. The concentration and purity of the purified DNA was then measured by using a NanoDrop 2,000 spectrophotometer (Thermo Fisher Scientific, Waltham, MA, USA). The C3435 T (rs1045642) polymorphism of the ABCB1 gene was determined using Real-Time Quantitative Polymerase Chain Reaction (qPCR) technique by TaqMan allelic discrimination assay. The sequence of the specific oligonucleotides used for amplification were as follows: Forward primer: 5'-TGC TGG TCC TGA AGT TGA TCT GTG AAC-3' and Reverse primer: 5'-ACA TTA GGC AGT GAC TCG ATG AAG GCA-3'. Two different fluorescently labeled minor groove binder (MGB) probes were used for allelic discrimination: the wild-type C allele was detected with the FAM-labeled probe (5'-FAM-GGA GAC CCA TCC C-MGB-3') and the mutant T allele was detected with the VIC-labeled probe (5'-VIC-GGA GAC TCA TCC C-MGB-3'). The qPCR amplification was performed on the ABI QuantStudio 5 Real-Time PCR System (Applied Biosystems, Foster City, CA, USA). The thermal cycling conditions were the following: initial denaturation was performed at 95 °C for 10 min, and subsequently denaturation was carried out at 95 °C for 15 s and annealing/extension at 60 °C for 1 min for 40 cycles. After the amplification, the endpoint fluorescence intensities of the FAM and VIC channels were measured. The specific genotypes (CC, CT or TT) were finally attributed on the basis of the clustering of the fluorescent signals with the assistance of allelic discrimination software of the system.

2.5 Machine learning model development

The data were split into a training set (70%) to derive the model, and a testing set (30%) to test the model, using the same random seed. Patients with missing values in the predefined clinical or experimental variables were excluded prior to modeling, negating the need for data imputation. To prevent data leakage between the training and testing sets, feature selection was conducted strictly within the training cohort using Least Absolute Shrinkage and Selection Operator (LASSO) regression with 10-fold cross-validation via the glmnet package. The optimal penalty parameter (lambda) was determined using the minimum binomial deviance criterion (lambda_min), retaining predictors with non-zero coefficients for subsequent modeling. Four different supervised machine learning algorithms were used for building predictive models for clinical efficacy: eXtreme Gradient Boosting (XGBoost), Random Forest (RF), Support Vector Machine (SVM), and Logistic Regression (LR). To prevent overfitting and account for model tuning uncertainty, a 5-fold cross-validation strategy combined with a systematic grid search was implemented strictly within the training cohort to optimize hyperparameters prior to final evaluation on the hold-out testing set. For the XGBoost model, the grid search evaluated max_depth (3, 4, 6), learning rate eta (0.01, 0.05, 0.1), subsample (0.7, 0.8, 1.0), and colsample_bytree (0.7, 0.8, 1.0); the final optimal configuration was max_depth=4, eta = 0.05, nrounds = 100, subsample = 0.8, colsample_bytree = 0.8, min_child_weight = 1, gamma = 0, and objective = "binary:logistic". For the Random Forest model, the optimal parameters were ntree = 500, mtry = 4 (number of variables randomly sampled at each split), and minimum nodesize = 5. For the SVM model, a radial basis function (RBF) kernel was utilized with an optimized cost parameter (C = 1.0) and gamma = 0.1. Standard multivariable Logistic Regression was fitted using maximum likelihood estimation without regularization.

Multidimensional clinical, TDM, and genetic data were combined to construct and compare the machine learning predictive models. Class weight adjustments were used to compensate for possible class imbalance problems of clinical data sets. In particular, we set scale_pos_weight in XGBoost to be inversely proportional to the frequency of classes, and class weighting in other algorithms to be inversely proportional to classes' sizes to avoid models favouring the positive class. Moreover, the SHapley Additive exPlanations (SHAP) method was combined with the best XGBoost model to visualize the interactions between LEV concentration and ABCB1 genotype. Specifically, the SHAP contribution matrix and the SHAP interaction values were used to extract the non-linear association of the clinical features and synergistic effect between them without assuming any biological causality.

2.6 Statistical analysis

All the statistical analyses and machine learning processes were performed using the R software. Shapiro–Wilk test was used to determine the distribution of the continuous variables. Normally distributed data were reported using mean and standard deviation (SD) and non-normally distributed data were reported as median and interquartile range (IQR). Kruskal–Wallis or Wilcoxon rank-sum tests were used to compare groups for continuous variables, as appropriate. Categorical data were summarized in terms of frequency and percentage, and compared using Chi-squared or Fisher's exact test, as appropriate. Receiver operating characteristic (ROC) curves were used to assess the discriminative ability of the models, and the areas under the curve (AUC) were compared using the DeLong

test. To quantify model uncertainty in the testing cohort, 95% confidence intervals (CIs) for AUCs were calculated via DeLong's method, and 95% CIs for classification metrics (sensitivity, specificity, precision, recall, and F1-score) were estimated using 1,000 stratified bootstrap replicates. To estimate clinical net benefit and predictive accuracy, decision curve analysis (DCA) and calibration curves were plotted. Statistically significant P values were set at < 0.05 (two sided).

3 Results

3.1 Baseline characteristics and population pharmacokinetics of levetiracetam

A total of 468 pediatric epilepsy patients receiving LEV therapy were initially screened from the institutional database. Of these, 122 patients (26.1%) were excluded based on the predefined criteria: 58 patients (12.4%) had incomplete baseline clinical, TDM, genotyping, or 6-month follow-up records (missing data); 34 patients (7.3%) had documented poor medication adherence; 21 patients (4.5%) had blood samples collected prior to reaching steady state or outside the 0.5-hour trough window; and 9 patients (1.9%) presented with baseline hepatic or renal dysfunction. Consequently, 346 patients fulfilled all eligibility criteria and were included in the final analysis, comprising 206 responders (59.5%) and 140 non-responders (40.5%) (the patient selection flow-chart is presented in Supplementary Figure S1). Table 1 shows the baseline demographic and clinical characteristics of the groups by clinical response. Interestingly, there was no significant difference in the daily dose of levetiracetam (LEV) per kg body weight between the two groups ($p = 0.924$). The non-responder group, on the other hand, had significantly lower LEV minimum steady-state concentration (Cmin) and concentration to dose ratio (CDR) than the responder group. Because LEV is predominantly eliminated unchanged via renal excretion, this finding is primarily explained by age-related differences in renal clearance: the non-responder group was significantly younger (mean age: 6.32 vs. 7.93 years, $P < 0.001$) and exhibited significantly lower serum creatinine (Scr) levels (40.77 vs. 44.65 umol/L, $P = 0.001$). In preschool and young children, kidney function (glomerular filtration rate) relative to body weight is substantially higher than in older children and adults, resulting in higher weight-normalized renal clearance and lower systemic exposure per kilogram of dose. Additionally, the more frequent use of concurrent enzyme-inducing anti-seizure medications (ASMs) (e.g., oxcarbazepine) in the non-responder group may have secondarily contributed to enhanced LEV elimination via non-hepatic enzymatic hydrolysis. Moreover, there was a significantly higher frequency of the TT genotype of the ABCB1 gene in non-responders.

Further population pharmacokinetic evaluation of LEV was done. The distribution of steady state Cmin in the cohort is shown in Figure 1A. The number of patients with concentrations outside the conventional reference interval (12–46 ug/mL) was substantial, and may indicate a potential need for localized targets for therapy in Chinese pediatric patients. When CDR was analyzed across age groups, younger children (particularly toddlers and preschool children under 3 and 3–6 years) exhibited significantly lower CDR values than older age groups (Figure 1B, $P < 0.001$). Notably, the distribution of concomitant ASMs did not differ significantly across the age groups (Chi-square test, $P = 0.482$), indicating that the lower CDR in younger children reflects their higher weight-normalized renal clearance rather than an unequal distribution of co-medications. Concomitant use of valproic acid was also a significant factor in LEV metabolism, with increased CDR, while levels were decreased with oxcarbazepine and carbamazepine use (Figure 1C). There was no significant difference in CDR among Han and other ethnic groups (Figure 1D). There was a positive correlation between the dose given and Cmin ($R = 0.72$, $p < 0.001$); however, the scatter plot highlighted a significant inter-individual variability (Figure 1E), which further supports the clinical need for therapeutic drug monitoring.

Across the entire cohort ($N = 346$), treatment-emergent adverse events were documented in 82 patients (23.7%), with no significant difference in overall incidence between responders and non-responders (22.8% vs. 25.0%, $P = 0.700$; Table 1). When categorized by specific clinical manifestation, the most frequently observed adverse events were neuropsychiatric and behavioral symptoms, including irritability or aggression in 36 patients (10.4%) and somnolence or fatigue in 25 patients (7.2%), followed by dizziness or headache in 12 patients (3.5%) and decreased appetite or gastrointestinal upset in 9 patients (2.6%). The theoretical therapeutic thresholds for this cohort were estimated by receiver operating characteristic (ROC) curve analysis (Figure 1F). An area under the curve (AUC) of 0.74 was obtained for the optimal Cmin cutoff value of 14.0 ug/mL, which was used to predict the clinical efficacy. In contrast, the AUC for the prediction of adverse events was only 0.53 and the threshold calculated was 17.6 ug/mL. The limited predictability for toxicity suggests that adverse events to LEV in children may be largely idiosyncratic and not concentration-related. This discovery suggests that such concentration monitoring is not enough for complete safety management and calls attention to the possible need to take account of other individualized parameters, such as genetic polymorphisms, in the clinical assessment.

3.2 Association of ABCB1 polymorphism with pharmacokinetics and clinical outcomes

Given that peripheral drug concentration might not be entirely predictive of the clinical consequences and adverse events as observed in Section 3.1, the influence of genetic variability in the ABCB1 gene, specifically C3435 T, was explored. The genotypic frequency distribution among the children is shown in Figure 2A, where 39.0%, 44.5%, and 16.5% of the children were identified as CC, CT, and TT, respectively. Weight-normalized doses were compared among the three genotypes at baseline to exclude possible genotype-dependent confounding factors, resulting from initial clinical decisions. No significant difference in prescribed doses was seen ($P = 0.936$) (Figure 2B), suggesting it is unlikely that the differences in clinical response were due to bias in prescribing the dose.

10.3389/fmed.2026.1914546

TABLE 1 Baseline characteristics and adverse event profiles of pediatric epilepsy patients in the whole population and categorized by clinical response.

Characteristics	Total (*n* = 346)	Responder (*n* = 206)	Non-responder (*n* = 140)	*P*-value
Age (years), mean (SD)	7.28 (3.80)	7.93 (3.63)	6.32 (3.86)	<0.001
Sex, *n* (%)				0.248
Female	165 (47.7)	104 (50.5)	61 (43.6)	
Male	181 (52.3)	102 (49.5)	79 (56.4)	
Ethnicity, *n* (%)				0.867
Han	309 (89.3)	183 (88.8)	126 (90.0)	
Others	37 (10.7)	23 (11.2)	14 (10.0)	
Weight (kg), mean (SD)	22.34 (8.03)	23.69 (7.74)	20.35 (8.06)	<0.001
Height (cm), mean (SD)	118.45 (23.12)	122.47 (21.91)	112.53 (23.66)	<0.001
BSA (m2), mean (SD)	0.85 (0.23)	0.89 (0.22)	0.79 (0.24)	<0.001
Epilepsy type, *n* (%)				0.427
Focal	199 (57.5)	117 (56.8)	82 (58.6)	
Generalized	125 (36.1)	73 (35.4)	52 (37.1)	
Unknown	22 (6.4)	16 (7.8)	6 (4.3)	
Therapy type, *n* (%)				0.011
Monotherapy	143 (41.3)	97 (47.1)	46 (32.9)	
Polytherapy	203 (58.7)	109 (52.9)	94 (67.1)	
Co-medication, *n* (%)				<0.001
None	143 (41.3)	97 (47.1)	46 (32.9)	
VPA	84 (24.3)	56 (27.2)	28 (20.0)	
OXC	87 (25.1)	35 (17.0)	52 (37.1)	
CBZ	32 (9.2)	18 (8.7)	14 (10.0)	
Formulation, *n* (%)				0.007
Oral solution	123 (35.5)	61 (29.6)	62 (44.3)	
Tablet	223 (64.5)	145 (70.4)	78 (55.7)	
Dosing frequency, *n* (%)				0.600
BID	323 (93.4)	194 (94.2)	129 (92.1)	
TID	23 (6.6)	12 (5.8)	11 (7.9)	
ALT (U/L), median [IQR]	26.00 [21.00, 34.00]	26.00 [21.00, 34.00]	26.00 [21.00, 33.00]	0.966
Scr (umol/L), mean (SD)	43.08 (10.64)	44.65 (10.29)	40.77 (10.77)	0.001
LEV daily dose (mg/d), mean (SD)	772.83 (353.86)	816.75 (344.93)	708.21 (358.28)	0.005
LEV dose (mg/kg/d), mean (SD)	34.64 (9.27)	34.60 (9.36)	34.69 (9.18)	0.924
LEV Cmin (ug/mL), median [IQR]	18.65 [14.62, 25.18]	19.79 [16.45, 25.87]	16.85 [12.55, 24.31]	<0.001
CDR, median [IQR]	0.59 [0.46, 0.70]	0.63 [0.51, 0.72]	0.53 [0.38, 0.66]	<0.001
ABCB1 genotype, *n* (%)				<0.001
CC	135 (39.0)	107 (51.9)	28 (20.0)	
CT	154 (44.5)	88 (42.7)	66 (47.1)	
TT	57 (16.5)	11 (5.3)	46 (32.9)	
Adverse event (overall), *n* (%)				0.700
No	264 (76.3)	159 (77.2)	105 (75.0)	
Yes	82 (23.7)	47 (22.8)	35 (25.0)	
Adverse event by type, *n* (%)				
Irritability/aggression	36 (10.4)	20 (9.7)	16 (11.4)	0.739
Somnolence/fatigue	25 (7.2)	15 (7.3)	10 (7.1)	1.000
Dizziness/headache	12 (3.5)	7 (3.4)	5 (3.6)	1.000
Decreased appetite/GI upset	9 (2.6)	5 (2.4)	4 (2.9)	1.000

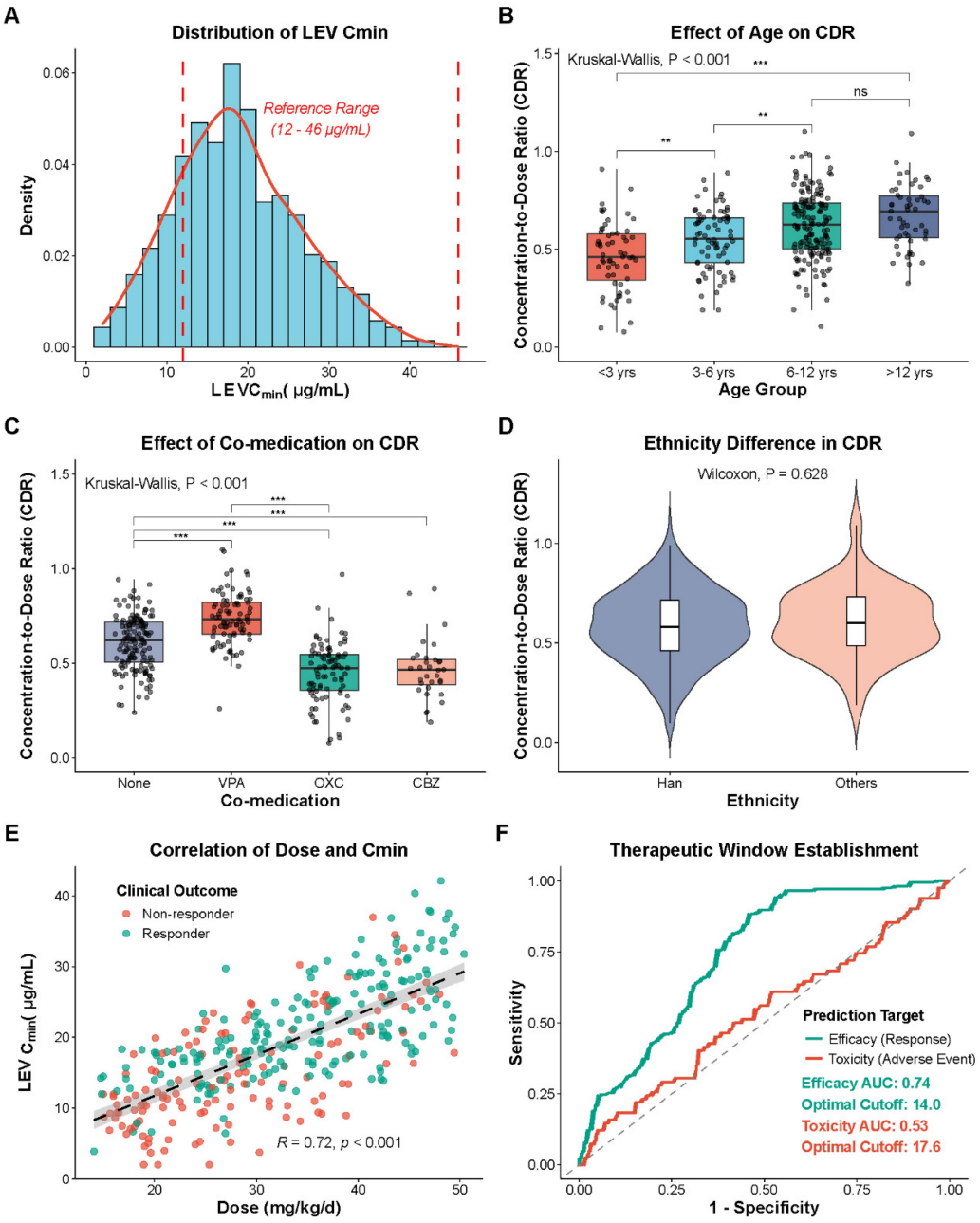


FIGURE 1
Population pharmacokinetic characteristics and therapeutic window analysis of levetiracetam (LEV). **(A)** Distribution of LEV minimum steady-state concentration C_{min}) in the study cohort. **(B)** Effect of age groups on the concentration-to-dose ratio (CDR). **(C)** Impact of concurrent antiseizure medications on CDR. **(D)** Distribution of CDR between different ethnicities. **(E)** Correlation between LEV dose and C_{min}, categorized by clinical outcomes. The dashed line indicates the linear regression fit. **(F)** Receiver operating characteristic (ROC) curves of C_{min} for predicting clinical efficacy and adverse events. Statistical differences were evaluated using the Kruskal–Wallis test **(B,C)** and Wilcoxon rank-sum test **(D)**.

The effects of the genotype of ABCB1 on systemic pharmacokinetics were then assessed. Interestingly, no significant difference was found in absolute LEV Cmin between the three genotypic groups (Figure 2C, $P = 0.094$). A slight difference was observed between the concentration to dose ratio (Figure 2D, $P = 0.041$), but the size of this change at the periphery is not likely to be large. This observation indicates that the ABCB1 C3435 T polymorphism does not substantially alter systemic LEV clearance in the peripheral circulation within our cohort.

The pharmacodynamic results by genotype showed significant differences as compared to the peripheral pharmacokinetic results. There was a significant difference in clinical responder rate between the wild-type CC group (79.3%) and the homozygous mutant TT group (19.3%) (Figure 2E, $P < 0.001$). At the same time, the rate of adverse events was significantly higher in the group of patients with TT genotype (45.6% vs. CC genotype 17.8%, Figure 2F, $P < 0.001$). Combining these observations suggests that while there is no difference in peripheral blood concentrations, patients with the TT mutation exhibit distinct clinical response rates. As a plausible biological hypothesis, this discrepancy might reflect genotype-related differences in blood-brain barrier transport or local central nervous system drug distribution, although indirect genetic associations

10.3389/fmed.2026.1914546

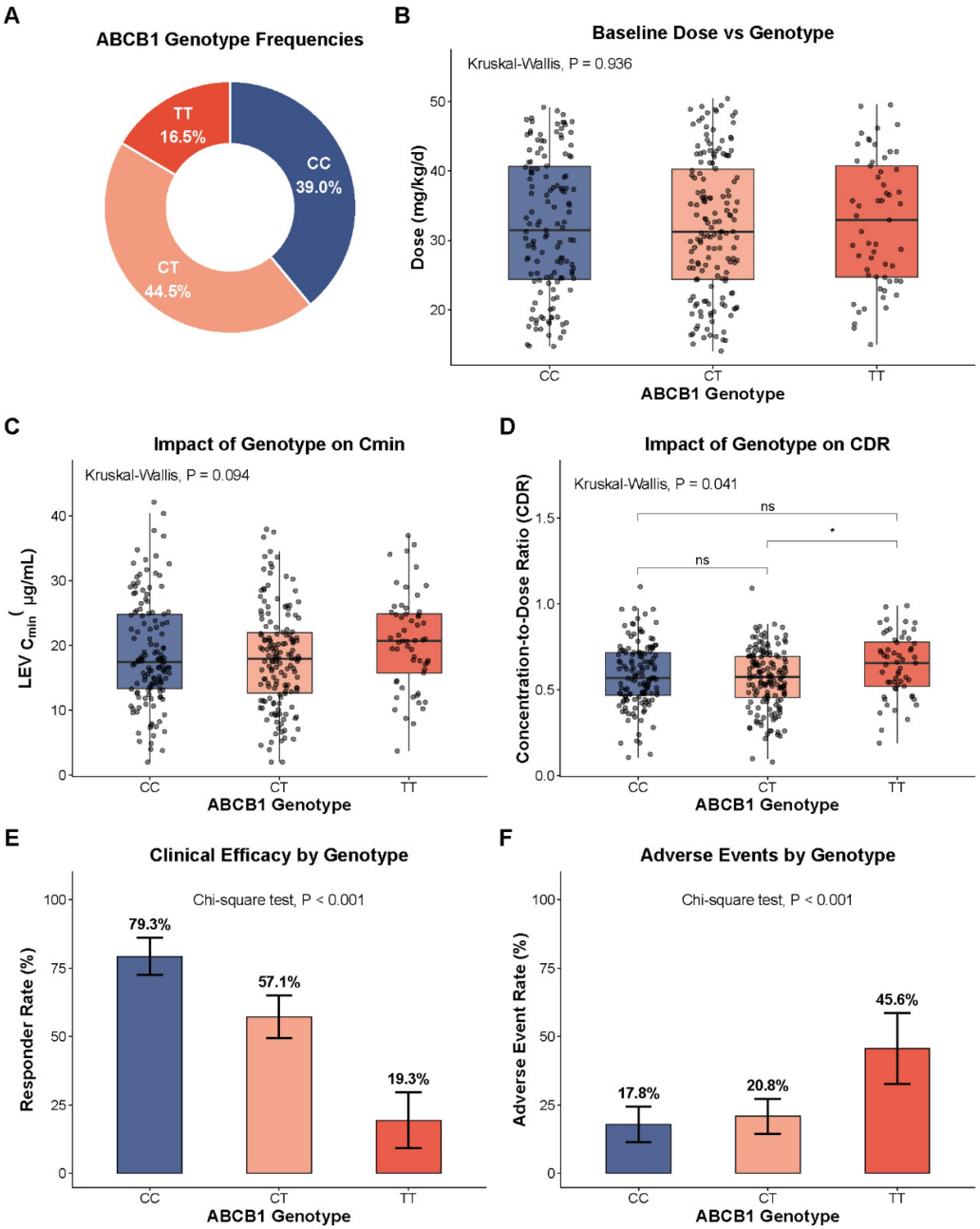


FIGURE 2
Distribution of the ABCB1 C3435 T genotype and its association with LEV pharmacokinetics and clinical outcomes. **(A)** Frequencies of ABCB1 genotypes in the cohort. **(B–D)** Comparisons of baseline dose **(B)**, LEV C_{min} **(C)**, and CDR **(D)** among patients with CC, CT, and TT genotypes. **(E, F)** Responder rate **(E)** and adverse event rate **(F)** stratified by ABCB1 genotype. Error bars in **(E)** and **(F)** represent the 95% confidence intervals. Statistical comparisons were performed using the Kruskal–Wallis test **(B–D)** and Chi-square test **(E,F)**.

cannot be excluded. Clinically, this divergence highlights the limitations of relying solely on peripheral therapeutic drug monitoring and supports the rationale for integrating genetic markers to improve treatment-response prediction.

3.3 Construction and evaluation of the machine learning predictive models

In the Spearman correlation analysis of the baseline predictors (Figure 3A), expected positive correlations were observed among anthropometric and demographic variables (such as age, height, weight, and BSA), whereas no severe multi-collinearity was detected between the primary experimental variables (LEV Cmin and ABCB1 genotype) and other clinical covariates. Subsequent LASSO regression coefficient path analysis in the training cohort (Figure 3B) identified the non-zero informative predictors—most notably LEV Cmin, ABCB1 genotype, therapy type, co-medication, age, and anthropometric indices—for inclusion in model training.

Later, four different machine learning algorithms namely XGBoost, Random Forest, Support Vector Machine (SVM) and Logistic Regression were trained and tested. The distribution of

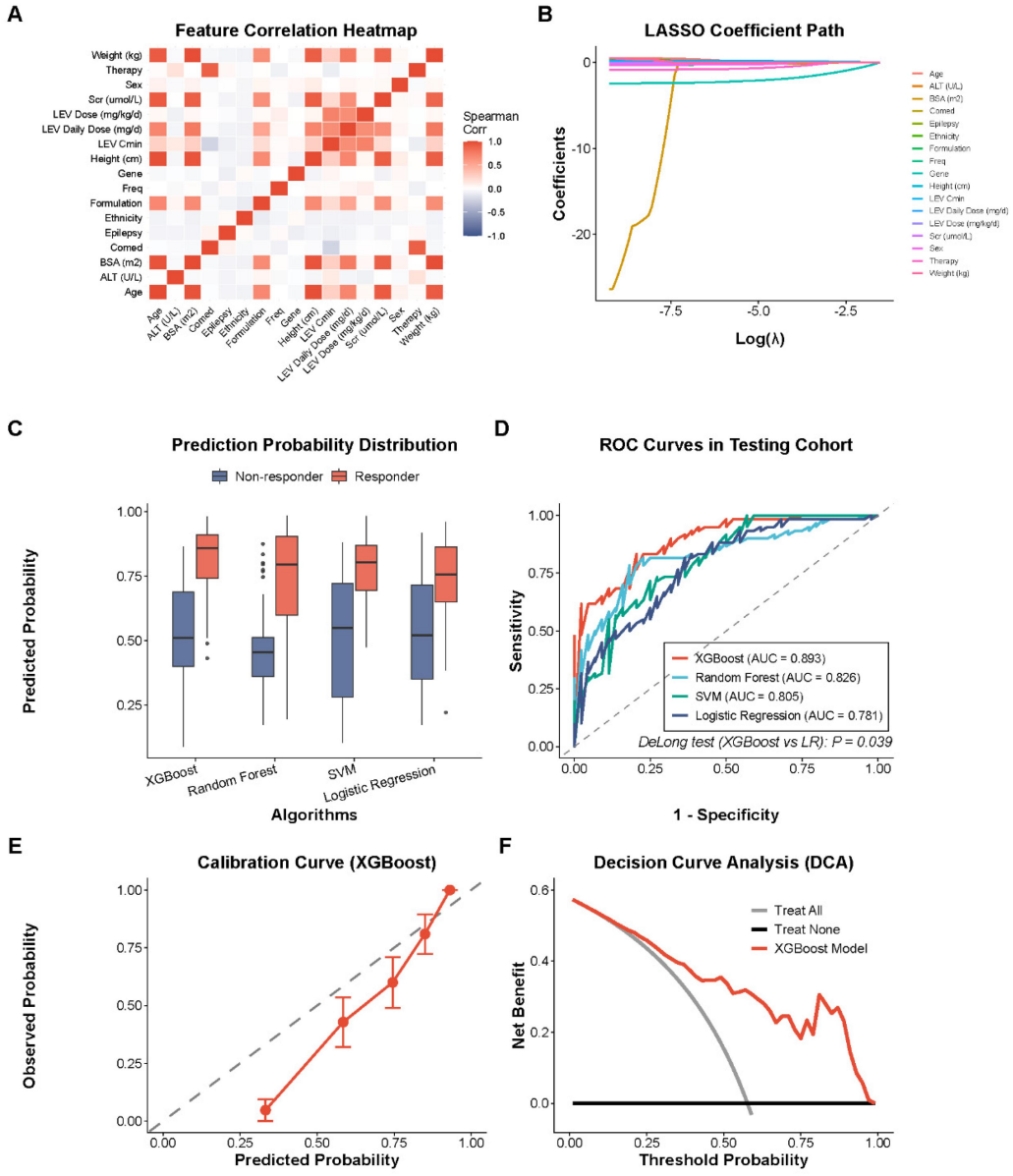


FIGURE 3
Construction and evaluation of the machine learning predictive models. **(A)** Spearman correlation heatmap of the included clinical and genetic features. **(B)** Least Absolute Shrinkage and Selection Operator (LASSO) coefficient path indicating the feature selection process. **(C)** Distribution of predicted probabilities generated by four machine learning algorithms, grouped by the actual clinical outcomes. **(D)** ROC curves of the four models in the testing cohort. The DeLong test was used to compare the AUC between the XGBoost and Logistic Regression models. **(E)** Calibration curve of the XGBoost model assessing the agreement between predicted and observed probabilities. **(F)** Decision curve analysis (DCA) estimating the net clinical benefit of the XGBoost model across different threshold probabilities.

the predicted probabilities for these models are shown in Figure 3C. The XGBoost model showed the most distinct separation between responders and non-responders. However, the traditional Logistic Regression model showed significant overlap between two groups in terms of predicted probabilities. This difference indicates that linear-model based approaches such as Logistic Regression might not be able to capture the intricate conditional relationships in the data (e.g., high levels of a drug might be beneficial in TT genotypes, but harmful in the wild-type patient outcomes), whereas tree-based algorithms can.

The discriminative performance was also objectively measured by Receiver Operating Characteristic (ROC) curves in the independent testing cohort (Figure 3D). To account for model uncertainty, 95% confidence intervals (CIs) were determined for all performance indicators. The XGBoost model achieved the highest Area Under the Curve (AUC) of 0.893 (95% CI: 0.831–0.955), followed by Random Forest at 0.826 (95% CI: 0.746–0.906) and SVM at 0.805 (95% CI: 0.721–0.889), while Logistic Regression yielded the lowest AUC of 0.781 (95% CI: 0.692–0.870). At the optimal Youden index cutoff point, the XGBoost model demonstrated a sensitivity (recall) of 0.855 (95% CI: 0.767–0.942), specificity of 0.810 (95% CI: 0.691–0.928), precision of 0.869 (95% CI: 0.784–0.954), and an F1-score of 0.862 (95% CI: 0.795–0.928). In contrast, the Logistic Regression

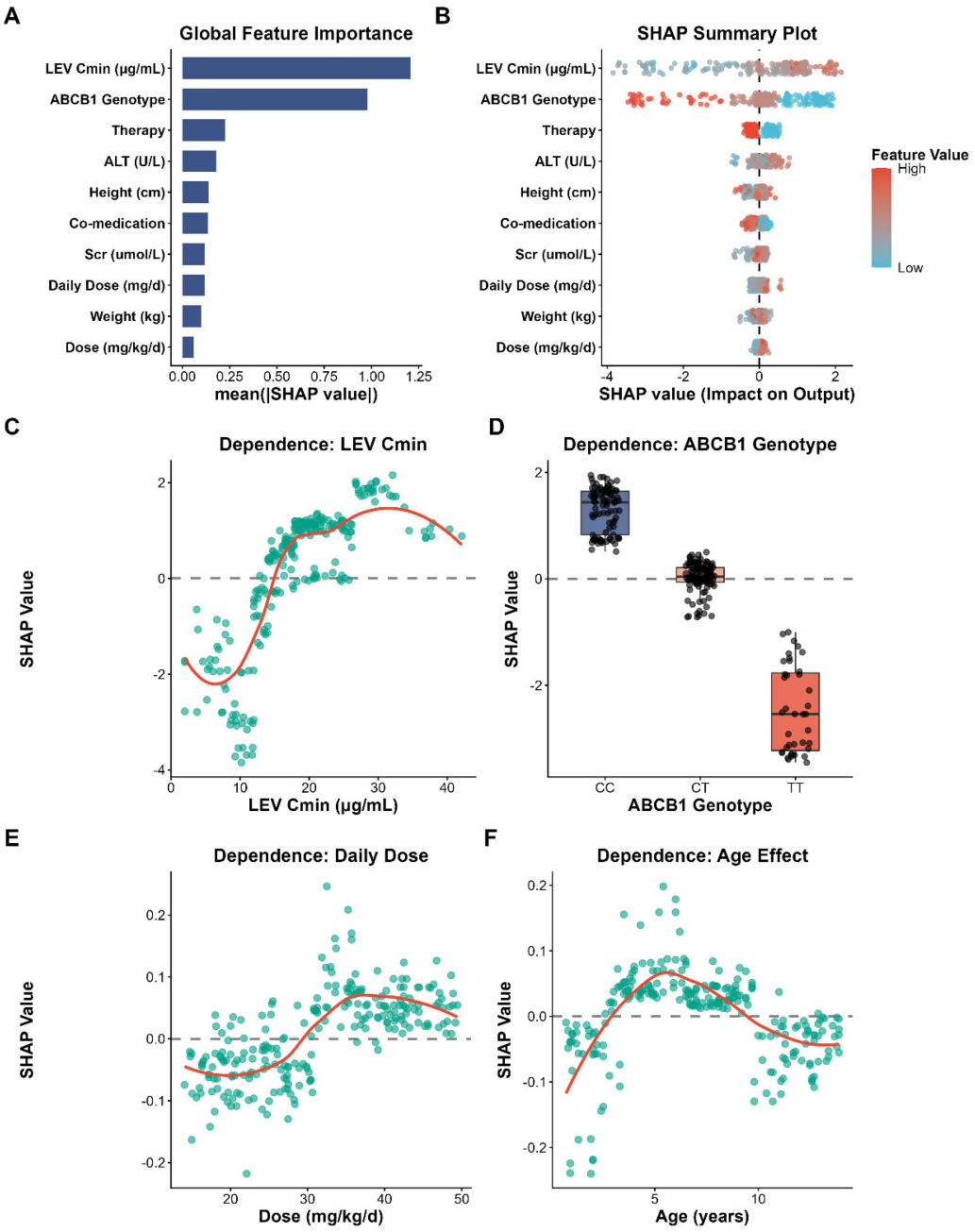


FIGURE 4
Model interpretability using SHapley additive exPlanations (SHAP) analysis. **(A)** Global feature importance ranked by the mean absolute SHAP values. **(B)** SHAP summary plot illustrating the distribution of SHAP values for individual features across all samples. Colors indicate the relative values of the features. **(C–F)** SHAP dependence plots showing the impact of LEV C_{min} **(C)**, ABCB1 genotype **(D)**, daily dose **(E)**, and age **(F)** on the model's output. The red lines in **(C)**, **(E)**, and **(F)** represent locally estimated scatterplot smoothing (LOESS) curves.

model exhibited lower overall performance metrics, with a sensitivity (recall) of 0.726 (95% CI: 0.615–0.837), specificity of 0.738 (95% CI: 0.605–0.871), precision of 0.804 (95% CI: 0.699–0.908), and an F1-score of 0.763 (95% CI: 0.675–0.851). Importantly, the DeLong test revealed that the increase of the AUC of the XGBoost model compared with the Logistic Regression model was statistically significant ($P = 0.039$), validating the methodological use of advanced machine learning for this particular clinical situation.

In addition to discriminative ability, reliability and clinical utility of the best model of XGBoost were evaluated. The calibration curve (Figure 3E) showed good agreement between the model-predicted probabilities and the observed frequencies of clinical response and did not show any systematic overestimation or underestimation of the model outcome. Finally, Decision Curve Analysis (DCA) was done to assess the clinical value of the model (Figure 3F). The DCA curve of the XGBoost model was always above the "Treat All" (assuming all patients require dosing interventions due to high risk of failure) and "Treat None" (assuming the standard empirical dose is sufficient for all patients without intervention) baselines with a wide spectrum of threshold probabilities, indicating that a

potential net clinical benefit may be achieved by using this model to predict treatment response and identify patients at high risk of therapeutic failure.

3.4 Model interpretability and non-linear associations via SHAP analysis

SHapley Additive exPlanations (SHAP) analysis was used to explain the underlying mechanisms behind the optimal XGBoost model in predicting the data. It is important to note that SHAP values represent mathematical associations and contributions of features in the predictive model and not necessarily direct biological causality. The global feature importance ranking (Figure 4A) showed that LEV Cmin and the genotype of ABCB1 were the most influential factors affecting the output of the model. This association was further clarified by the SHAP summary plot (Figure 4B), which shows that the associations of higher LEV Cmin were mainly towards positive SHAP values (increase in likelihood of efficacy) and the presence of the ABCB1 TT genotype were mainly towards negative SHAP values (decrease in likelihood of efficacy).

The SHAP dependence plots gave insights into non-linear relationships between specific features and clinical outcomes. In the case of LEV Cmin (Figure 4C), the locally estimated scatterplot smoothing (LOESS) curve showed a clearly defined threshold effect. SHAP values rose sharply with each increase in Cmin from ~15–30 ug/mL and corresponded to an increase in the probability of therapeutic response. At concentrations > 30–35ug/mL however, a plateau was reached and a downward trend was observed. This decrease can be related to beginning of the dose dependent adverse events clinically expressed as the failure or intolerance of treatment. Moreover, dependence plot for ABCB1 genotype (Figure 4D) showed that positive predictive contribution was always associated with the wild-type CC genotype, while the homozygous TT mutation correlated greatly with a negative impact on efficacy prediction.

In addition, dependence plots for the nominal daily dose (Figure 4E) and patient age (Figure 4F) were assessed. Non-linear trends were found, for example a peak at 5–8 years of age in predictive contribution followed by a decline but the magnitude of the impact of these trends is not to be easily interpreted. One important point when comparing the *y*-axis scales is that the absolute values of SHAP for administered dose and age were very similar and in a very small range (around −0.2 and close to +0.2). Actual blood concentration and genotype, on the other hand, were much more influential (between −4.0 and +2.0). This significant scale mismatch is not an over-interpretation of weak features, but rather a vital clinical principle: standard weight-based dosing and age are relatively poor predictors of the eventual clinical outcome when compared to the actual systemic exposure that is obtained and the genetic profile of the patient. Based on these results, individualized therapeutic strategies might benefit from the monitoring of Cmin and genetic profiling rather than relying solely on the traditional empirical approach of dosing.

3.5 SHAP interaction analysis and individualized clinical prediction

Based on the results of non-linear main effects, SHAP interaction matrices were used to examine the mathematical association of pharmacokinetics and genetic polymorphisms in combination. Figure 5A shows the interaction of LEV Cmin with genotype of ABCB1. The LOESS smoothing curves suggest that the ABCB1 genotype may modify the associative relationship between systemic exposure and model-predicted response. Specifically, for patients with the wild-type CC genotype (blue line), the combined SHAP contribution crossed zero into the positive range at a comparatively lower Cmin. By contrast, the curve for the homozygous TT mutation (red line) remained in the negative SHAP range across moderate concentrations and only shifted toward positive mathematical contributions at higher observed Cmin values. The interaction of nominal dose and genotype is shown in Figure 5B. A similar trend was seen, however, the SHAP interaction values for dose were substantially lower, consistent with the results in Section 3.4 and again highlighting the importance of systemic exposure compared to nominal dose. Because SHAP values represent mathematical contributions to model predictions rather than clinically validated cutoffs, these interaction patterns should be interpreted as an exploratory hypothesis that the exposure-response relationship may vary by genotype, rather than as established genotype-specific therapeutic target concentrations.

In order to illustrate the clinical applicability of the model for individual patient decision making, waterfall plots of SHAP were created for four representative patient scenarios. Figure 5C shows the profile of Patient A, a typical successful case, in which the synergistic positive effects of the CC genotype and a typical Cmin (19.6 ug/mL) resulted in a prediction of clinical efficacy. Patient B is shown in Figure 5D, which depicts a case of genetic resistance. Although, it attained a nominal dose and Cmin similar to Patient A, the presence of the TT genotype had a huge negative effect on the output of the model, pushing the overall prediction towards treatment failure.

Patient C is shown in Figure 5E, illustrating an observed case of a TT carrier who achieved clinical response in the presence of a high steady-state LEV Cmin (32.1 ug/mL). Within the model's mathematical structure, the negative SHAP contribution associated with the TT genotype was counterbalanced by the positive contribution of the higher observed LEV Cmin. Finally, Figure 5F illustrates Patient D, a patient who was failing subtherapeutically. In this case the patient had a very low Cmin (2.0 ug/mL). The model was able to assign the greatest negative penalty to this very poor systemic exposure, and thus to predict treatment failure, while taking other clinical factors into consideration. The evaluation of Patient D shows that the machine learning algorithm follows the basic principles of pharmacology, which suggests that the model remains robust even in extreme clinical presentations. Together, these individual case decompositions illustrate how the model integrates TDM and ABCB1 genotype to estimate treatment-response probabilities, generating hypotheses for future prospective exposure-response studies rather than serving as a direct rule for dose adjustment.

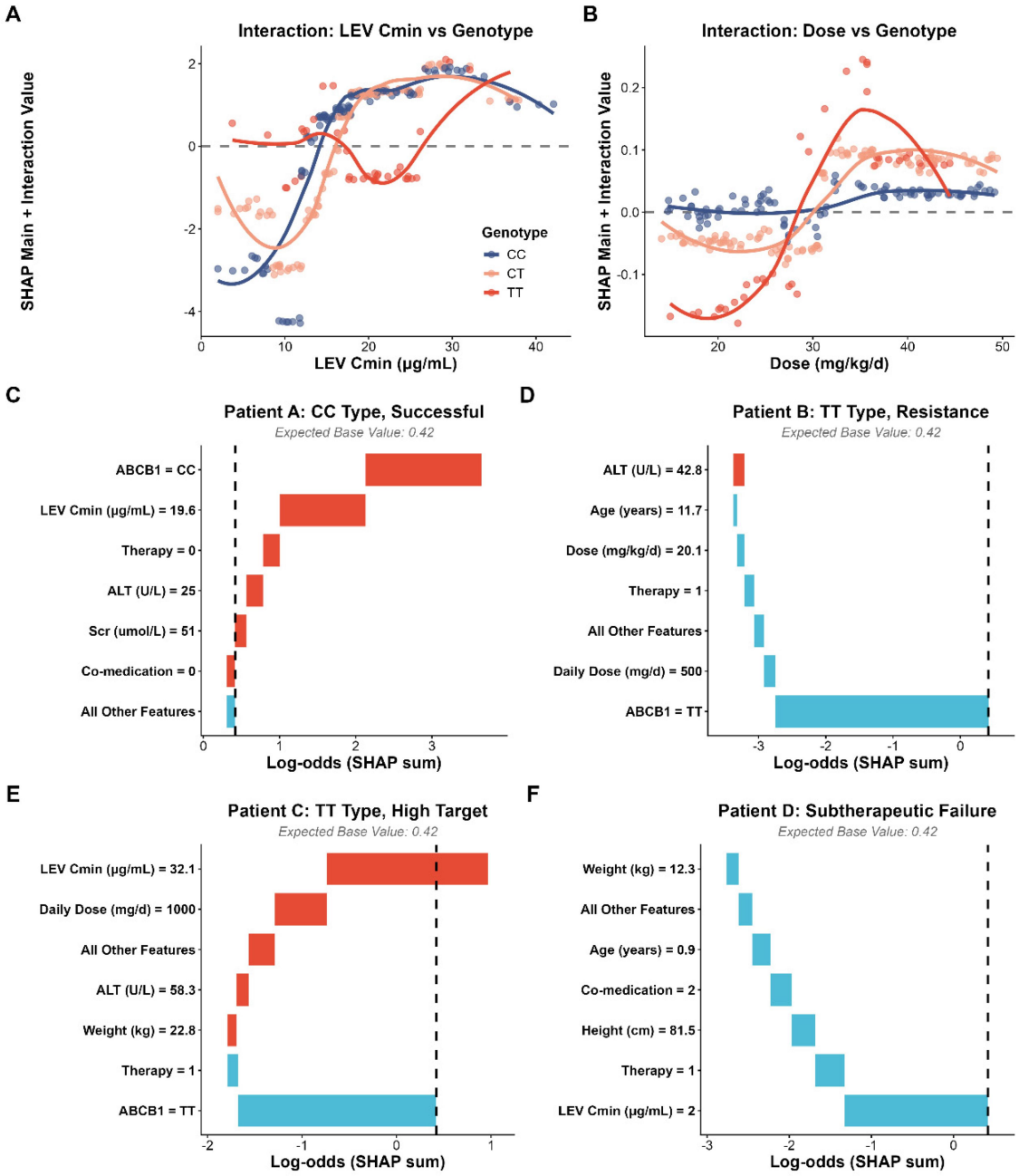


FIGURE 5
SHAP interaction analysis and individualized prediction for representative patients. **(A,B)** SHAP interaction plots demonstrating the combined effects of ABCB1 genotype with LEV C_{min} **(A)** and dose **(B)** The LOESS curves indicate the trend of SHAP main and interaction values for each genotype. **(C–F)** SHAP waterfall plots detailing the individualized prediction process for four representative cases: a successful CC-type patient **(C)**, a resistant TT-type patient **(D)**, a TT-type patient with a high target concentration **(E)**, and a patient experiencing subtherapeutic failure **(F)** Red bars denote positive contributions to the prediction of efficacy, while blue bars denote negative contributions.

4 Discussion

The broad inter-individual variation in the pharmacokinetics of levetiracetam in children can make empirical weight-based dosing difficult, and emphasizes the necessity of precision medicine approaches. In this study, we designed a machine learning-based treatment-response prediction model using therapeutic drug monitoring and ABCB1 C3435 T genetic polymorphism. It should be explicitly noted that this model predicts the probability of binary clinical response under a given set of clinical characteristics and systemic exposure levels, rather than directly outputting an individualized dose regimen; however, its associative insights may help identify patients at risk of poor response compared to conventional evaluation methods.

Several different reference intervals of levetiracetam concentrations have been suggested in the literature before, with a low reference value ranging from 12 to 46 μg/mL for effective seizure control (13). These are general pharmacokinetics guidelines and in our cohort the optimum efficacy threshold

was estimated at 14.0ug/mL. One caveat to our results, however, is that the peripheral trough concentration was not very predictive of adverse events (AUC, 0.53). This is unlikely a methodological problem, but rather is consistent with the neuropharmacological reports of neurobehavioral toxicities of levetiracetam in children being largely idiosyncratic. This suggests that adverse events are not directly concentration-dependent, and thus reasonably accounts for the lack of effectiveness of conventional therapeutic drug monitoring for safety management, and underscores the need for genetic biomarkers.

The addition of the ABCB1 C3435 T polymorphism gave much insight to pharmacodynamic differences. Responder rate was significantly lower for patients with a TT genotype and adverse events occurred significantly more often in patients with a TT genotype. Whether these differences in outcome are due to differences in the baseline dosing is questionable. The baseline analysis showed that weight-normalized administered doses were nearly identical between the two groups ($P = 0.924$), whereas trough concentrations and CDR were lower in the non-responder group. Because LEV is predominantly excreted unchanged by the kidneys, this lower systemic exposure is primarily explained by the younger age and lower serum creatinine levels observed in the non-responder group, reflecting the heightened weight-normalized glomerular filtration rate and renal drug clearance characteristic of preschool children, alongside a secondary contribution from concurrent enzyme-inducing ASMs such as oxcarbazepine (14). Furthermore, it is plausible that the higher clinical failure rate observed in TT carriers could be partially confounded by an uneven distribution of these enzyme-inducing co-medications. Nevertheless, the machine learning algorithm inherently adjusts for such multivariable interactions, and the SHAP analysis continued to identify the TT mutation as a strong, independent associative factor for negative outcomes. More importantly, there were no significant differences in the absolute peripheral concentrations between the three genotypes. In the literature, the mechanistic role of ABCB1/P-glycoprotein in LEV transport remains incompletely established; while rodent models have suggested P-gp-mediated transport of LEV, *in vitro* studies utilizing human P-gp-transfected cell lines have reported weak or absent directional transport (15). Therefore, the hypothesis that the ABCB1 C3435 T polymorphism alters P-glycoprotein expression at the blood-brain barrier and modifies local central nervous system LEV exposure without changing peripheral blood levels should be viewed as a plausible biological hypothesis rather than a proven causal mechanism demonstrated by the present study. It is also possible that C3435 T is in linkage disequilibrium with other functional variants or reflects broader pharmacodynamic susceptibility in refractory epilepsy.

A machine learning framework was used to process these complex interactions. In the testing cohort, the XGBoost algorithm performed notably better than logistic regression. Such a performance difference suggests that linear models may not be appropriate for representing clinically non-linear conditional logic (16), as a high concentration may be beneficial for TT carriers, and become toxic for the wild-type. SHAP analysis was used to explain these patterns. It should be emphasized that the value of SHAP component in a model is not a direct biological causality but a mathematical association, and the contribution of the component is highlighted (17). While the SHAP interaction plots showed that positive model predictions in TT carriers were mathematically associated with higher observed Cmin values compared to CC carriers, this observation does not prove that TT carriers physiologically require a higher therapeutic trough concentration, nor should SHAP curves be interpreted directly as clinically validated therapeutic thresholds. Demonstrating whether TT carriers truly benefit from a higher target Cmin would require formal quantitative exposure-response modeling and prospective validation through structured dose adjustments and subsequent clinical outcome assessments. Therefore, our SHAP interaction findings are presented strictly as a hypothesis requiring further verification rather than as an established basis for clinical dose adjustment. The personalized waterfall plots further highlighted the potential of incorporating these 'associative features' to guide clinical evaluation in a dynamic fashion, thereby linking the population statistics and personalized medicine.

The present study has some limitations. First, this is a single center retrospective study relying on a single 70:30 training-testing split without independent external validation, and the geographic and ethnic profile of the cohort might limit the generalizability of the proposed predictive model. Although the XGBoost model achieved a relatively high internal AUC, this metric strictly reflects discriminative ability within the current dataset and does not establish that the algorithm can safely guide individualized dose adjustments in clinical practice. Additionally, even though we excluded patients with documented poor adherence and restricted TDM measurements to the initial steady-state maintenance phase, relying on a single initial Cmin measurement without serial longitudinal TDM controls during the 6-month follow-up cannot fully account for intra-individual pharmacokinetic variations over time (such as somatic growth or unrecorded minor adherence fluctuations), and retrospective observational data remain inherently susceptible to selection and information biases. Rigorous external validation in large, multicenter prospective cohorts is mandatory before this predictive framework could be considered for clinical decision support. Second, other possible genetic polymorphisms affecting the pharmacodynamics and pharmacokinetics of levetiracetam (such as SV2A genetic variants) were not considered, indicating that there may be other unmeasured confounder factors. Third, while the overall sample size was sufficient for initial model training, the subgroup of patients with the homozygous TT mutation was relatively small ($n = 57$). This limited sample size may constrain the statistical robustness of the specific SHAP interaction thresholds proposed for TT carriers, highlighting the need for larger cohorts to substantiate these associative findings.

5 Conclusion

The aim of this study was to obtain a treatment-response prediction model for levetiracetam in pediatric epilepsy patients through combination of TDM and ABCB1 C3435 T genetic polymorphism using machine learning techniques. These associative factors were shown to be important when using the XGBoost algorithm, which, in combination with SHAP analysis,

demonstrated that the ABCB1 TT genotype and actual systemic exposure (Cmin) were important factors for prediction of clinical outcomes, compared with nominal weight-based dosing. Rather than establishing a direct individualized dosing regimen or clinically validated concentration cutoffs, our SHAP interaction analyses generate the exploratory hypothesis that ABCB1 genotype may modify the relationship between systemic LEV exposure and clinical response. Because the current findings are derived from a single-center retrospective cohort with a limited TT subgroup size and lack external validation, they do not provide sufficient evidence to directly guide clinical dose adjustments. Future quantitative exposure-response modeling and multicenter prospective trials are essential to verify these hypotheses before clinical implementation.

Data availability statement

The raw data supporting the conclusions of this article will be made available by the authors, without undue reservation.

Ethics statement

The studies involving humans were approved by Institutional Review Board of Panzhihua Central Hospital. The studies were conducted in accordance with the local legislation and institutional requirements. Written informed consent for participation was not required from the participants or the participants' legal guardians/next of kin in accordance with the national legislation and institutional requirements.

Author contributions

XL: Conceptualization, Data curation, Formal analysis, Funding acquisition, Investigation, Methodology, Project administration, Software, Supervision, Writing – original draft, Writing – review & editing. LZ: Conceptualization, Data curation, Formal analysis, Investigation, Methodology, Software, Writing – original draft. JC: Conceptualization, Data curation, Investigation, Software, Writing – original draft. FS: Conceptualization, Data curation, Investigation, Software, Writing – original draft. ZY: Conceptualization, Data curation, Investigation, Software, Supervision, Writing – review & editing.

Funding

The author(s) declared that financial support was received for this work and/or its publication. Research Project of the National Health Commission (Grant Nos. GWJJMB202510025013, YLZLXZ24G039); the General Program of the Natural Science Foundation of Sichuan Province (Grant No. 2025ZNSFSC0684); the General Program of the Local University Joint Special Fund of the Department of Science and Technology of Yunnan Province (Grant No. 202001BA070001-041); the Key Project of the Open Fund of the Yunnan Provincial Key Laboratory of Pharmacology for Natural Products (Grant Nos. YKLPNP-K2302, YKLPNP-K2504); the Young Pharmacist Scientific Research Special Fund of the Sichuan Hospital Association (Grant Nos. 22009, YP2202419); the Scientific Research Project of the Sichuan Society for Medical Science and Technology Innovation (Grant No. 2025YCYM107); the Pharmaceutical Scientific Research Project of the Chengdu Pharmaceutical Association (Grant Nos. Cdyxky7021, Cdyxky8041); the Project of the Panzhihua Municipal Science and Technology Bureau (Grant No. 2024ZD-S-28); and the Intramural Research Project of Panzhihua Central Hospital (Grant No. 202311).

Conflict of interest

The author(s) declared that this work was conducted in the absence of any commercial or financial relationships that could be construed as a potential conflict of interest.

Generative AI statement

The author(s) declared that generative AI was not used in the creation of this manuscript.

Any alternative text (alt text) provided alongside figures in this article has been generated by Frontiers with the support of artificial intelligence and reasonable efforts have been made to ensure accuracy, including review by the authors wherever possible. If you identify any issues, please contact us.

Publisher's note

All claims expressed in this article are solely those of the authors and do not necessarily represent those of their affiliated organizations, or those of the publisher, the editors and the reviewers. Any product that may be evaluated in this article, or claim that may be made by its manufacturer, is not guaranteed or endorsed by the publisher.

Supplementary material

The Supplementary Material for this article can be found online at: https://www.frontiersin.org/articles/10.3389/fmed.2026.1914546/full#supplementary-material

References

1. Zhang M, Jin Y, Li W, He C, Di X, Duan Y, et al. Quantitation of levetiracetam concentrations in plasma and saliva samples by ultra-performance liquid chromatography-tandem mass spectrometry: application to therapeutic drug monitoring for pregnant women with epilepsy. *Biomed Chromatogr*. (2024) 38: e5777. doi: 10.1002/bmc.5777

2. Sourbron J, Chan HY, Wammes-van der Heijden EA, Klarenbeek P, Wijnen BFM, De Haan G-J, et al. Review on the relevance of therapeutic drug monitoring of levetiracetam. *Seizure*. (2018) 62:131–5. doi: 10.1016/j.seizure.2018.09.004

3. Yamamoto Y, Ohta A, Usui N, Imai K, Kagawa Y, Takahashi Y. Clinical value of therapeutic drug monitoring for levetiracetam in pediatric patients with epilepsy. *Brain Dev*. (2023) 45:285–92. doi: 10.1016/j.braindev.2023.01.007

4. Sheinberg R, Heyman E, Dagan Z, Youngster I, Kohn E, Gandelman-Marton R, et al. Correlation between efficacy of levetiracetam and serum levels among children with refractory epilepsy. *Pediatr Neurol*. (2015) 52:624–8. doi: 10.1016/j.pediatrneurol.2015.01.012

5. Iwasaki T, Toki T, Nonoda Y, Ishii M. The efficacy of levetiracetam for focal seizures and its blood levels in children. *Brain Dev*. (2015) 37:773–9. doi: 10.1016/j.braindev.2014.11.008

6. Loscher W, Potschka H. Drug resistance in brain diseases and the role of drug efflux transporters. *Nat Rev Neurosci*. (2005) 6:591–602. doi: 10.1038/nrn1728

7. Baltes S, Gastens AM, Fedrowitz M, Potschka H, Kaever V, Loscher W. Differences in the transport of the antiepileptic drugs phenytoin, levetiracetam and carbamazepine by human and mouse P-glycoprotein. *Neuropharmacology*. (2007) 52:333–46. doi: 10.1016/j.neuropharm.2006.07.038

8. Potschka H, Baltes S, Loscher W. Inhibition of multidrug transporters by verapamil or probenecid does not alter blood-brain barrier penetration of levetiracetam in rats. *Epilepsy Res*. (2004) 58:85–91. doi: 10.1016/j.eplepsyres.2003.12.007

9. Methaneethorn J, Duangchaemkarn K, Reisfeld B, Habiballah S. Methodological techniques used in machine learning to support individualized drug dosing regimens based on pharmacokinetic data: a scoping review. *Clin Pharmacokinet*. (2025) 64:1295–330. doi: 10.1007/s40262-025-01547-8

10. Bruce JL. An overview of supervised machine learning in drug discovery, PK/PD modeling and precision pharmacogenomics. *Medi Clin Case Rep J*. (2025) 3:1439–45. doi: 10.51219/MCCRJ/Julian-Lloyd-Bruce/406

11. Abdaltawab A, Chang LC, Mansour M, Koubeissi M. How accurate are machine learning models in predicting anti-seizure medication responses: a systematic review. *Epilepsy Behav*. (2025) 163:110212. doi: 10.1016/j.yebeh.2024.110212

12. Lundberg SM, Erion G, Chen H, DeGrave A, Prutkin JM, Nair B, et al. From local explanations to global understanding with explainable AI for trees. *Nat Mach Intell*. (2020) 2:56–67. doi: 10.1038/s42256-019-0138-9

13. Patsalos PN, Berry DJ, Bourgeois BFD, Cloyd JC, Glauser TA, Johannessen SI, et al. Antiepileptic drugs–best practice guidelines for therapeutic drug monitoring: a position paper by the subcommission on therapeutic drug monitoring, ILAE commission on therapeutic strategies. *Epilepsia*. (2008) 49:1239–76. doi: 10.1111/j.1528-1167.2008.01561.x

14. Contin M, Albani F, Riva R, Baruzzi A. Levetiracetam therapeutic monitoring in patients with epilepsy: effect of concomitant antiepileptic drugs. *Ther Drug Monit*. (2004) 26:375–9. doi: 10.1097/00007691-200408000-00006

15. Gericke B, Borsdorf S, Wienboker I, Noack A, Noack S, Loscher W. Similarities and differences in the localization, trafficking, and function of P-glycoprotein in MDR1-EGFP-transduced rat versus human brain capillary endothelial cell lines. *Fluids Barriers CNS*. (2021) 18:36. doi: 10.1186/s12987-021-00266-z

16. Ha C, Lee H-S, Joo EY, Shon Y-M, Hong SB, Seo D-W, et al. Levetiracetam therapeutic drug monitoring in a large cohort of Korean epileptic patients. *Pharmaceuticals (Basel)*. (2021) 14:826. doi: 10.3390/ph14080826

17. Besag FMC, Vasey MJ, Sen A. Current evidence for adjunct pyridoxine (vitamin B6) for the treatment of behavioral adverse effects associated with levetiracetam: a systematic review. *Epilepsy Behav*. (2023) 140:109065. doi: 10.1016/j.yebeh.2022.109065